Reconstitution of Blue−Green Reversible Photoconversion of a Cyanobacterial Photoreceptor, PixJ1, in Phycocyanobilin-Producing *Escherichia coli*†

Shizue Yoshihara,‡ Takashi Shimada,§ Daisuke Matsuoka,‡ Kazunori Zikihara,‡,|| Takayuki Kohchi,⊥ and Satoru Tokutomi*,‡

Department of Biological Science, Graduate School of Science, Osaka Prefecture University, 1-1 Gakuen-cho, Sakai, Osaka 599-8531, Japan, Tsukuba Proteomics Research Center, SHIMADZU BIOTECH, 3-17-1 Azuma, Tsukuba 305-0031, Japan, Division of Integrated Life Science, Graduate School of Biostudies, Kyoto University, Sakyo-ku, Kyoto 606-8502, Japan, and Radiation Biology Center, Kyoto University, Sakyo-ku, Kyoto 606-8501, Japan

Received September 30, 2005; Revised Manuscript Received January 20, 2006

ABSTRACT: PixJ1, a photoreceptor in the unicellular cyanobacterium *Synechocystis* sp. PCC 6803, mediates positive phototactic motility and contains two GAF domains, the latter of which binds a bilin chromophore. Full-length PixJ1 expressed and purified from *Synechocystis* showed unique reversible photoconversion between a blue light-absorbing (Pb) form and a green light-absorbing (Pg) form (*1*) in contrast to the reversible phototransformation between the red light-absorbing form and far-red light-absorbing form of the other GAF-containing photoreceptors such as plant or bacterial phytochromes. To clarify the origin of the blue-shifted photoconversion, we tried to reconstitute this blue−green reversible phototransformation by synthesizing the second GAF domain in *Escherichia coli* transformed with genes for biosynthesis of four different bilins, biliverdin (BV), bilirubin (BR), phycocyanobilin (PCB), and phycocyanorubin (PCR), as final products. The three expression systems, the BR system being the exception, produced a GAF polypeptide with a covalently bound bilin. The GAF polypeptide from the BV-synthesizing system exhibited an irreversible photoconversion, while that from the PCB-synthesizing system revealed photoconversion between Pb and Pg almost identical to that of the full-length PixJ1, indicating that PCB is responsible for the blue−green reversible photoconversion. Furthermore, the GAF polypeptide from the PCR-producing system exhibited almost the same reversible spectral change, possibly coming from the PCB accumulated in the PCR-biosynthetic pathway. Mass spectrometry (MS) of the main tryptic chromopeptide revealed that the chromophore binds to a 21-amino acid peptide that contains a cysteine-histidine motif for phytochrome chromophore binding and that an ion signal can be assigned to desorbed PCB. The absorption spectra of the denatured GAF polypeptide suggested that PCB is attached to the protein moiety in a twisted conformation that disrupts the π-electron conjugation between the A and B rings, possibly being held in position through a second covalent linkage.

Plants use visible light to sense their environmental conditions to fine-tune their development as well as to produce energy in photosynthesis. Plants have acquired two types of photoreceptors for this purpose, phytochrome and the blue light photoreceptors. Plant phytochromes are soluble chromoproteins composed of ~1100 amino acid residues and bind one linear tetrapyrrole chromophore, phytochromobilin (PΦB),[1] covalently attached to a conserved Cys residue through a thioether linkage, and mediate a broad range of photomorphogenetic responses such as seed germination, de-etiolation, and floral induction (*2*, *3*). They exist in two forms, namely, the red light-absorbing (Pr) and the far-red light-absorbing (Pfr) forms that can be reversibly interconverted by red or far-red light, and act as a light-regulated molecular switch.

With recent developments in genomic science, distinct homologues of plant phytochrome, known as bacteriophytochromes, have been found in many prokaryotic organisms, such as Cph1 from the unicellular cyanobacterium *Synechocystis* sp. PCC 6803 (*4*), CphA from the filamentous cyanobacterium *Calothrix* sp. PCC 7601 (*5*), and BphPs from the soil bacterium *Agrobacterium tumefaciens* (*6*), the pathogenic bacterium *Pseudomonas aeruginosa* (*7*), and the

† This work was supported by grants-in-aid from MEXT Japan to S.Y. (17770041) and S.T. (13139205 and 17084008).

* To whom correspondence should be addressed. Phone: +81-72-254-9841. Fax: +81-72-254-9841. E-mail: toxan@b.s.osakafu-u.ac.jp.

‡ Osaka Prefecture University.

§ SHIMADZU BIOTECH.

|| Radiation Biology Center, Kyoto University.

⊥ Division of Integrated Life Science, Graduate School of Biostudies, Kyoto University.

[1] Abbreviations: Pb, blue light-absorbing form; Pg, green light-absorbing form; Pr, red light-absorbing form; Pfr, far-red light-absorbing form; PCB, phycocyanobilin; PCR, phycocyanorubin; PEB, phycoerythrobilin; PUB, phycourobilin; PVB, phycoviolobilin; PΦB, phytochromobilin; BR, bilirubin; BV, biliverdin IXα; BvdR, biliverdin reductase; HO, heme oxygenase; PcyA, phycocyanobilin:ferredoxin oxidoreductase; PecA, α-subunit of phycoerythrocyanin; pR, phoborhodopsin; GST, glutathione *S*-transferase; DMSO, dimethyl sulfoxide; PAGE, polyacrylamide gel electrophoresis; HPLC, high-performance liquid chromatography; MS, mass spectrometry; MALDI-TOF, matrix-assisted laser desorption ionization time-of-flight; MALDI-QIT-TOF, matrix-assisted laser desorption ionization quadrupole ion trap time-of-flight; λ_{max}, absorption maximum; TFA, trifluoroacetic acid.

10.1021/bi051983l CCC: $33.50
Published on Web 02/14/2006

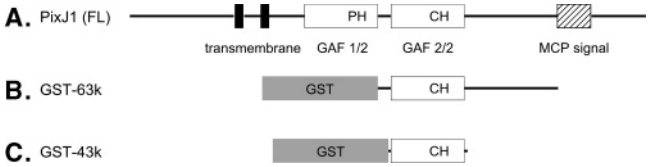

FIGURE 1: Domain structure and recombinant polypeptides of *Synechocystis* sp. PCC 6803 PixJ1. (A) Domain and motif structure of PixJ1. FL, GAF 1/2, and MCP represent the full-length protein, the first GAF domain from the N-terminus, and the methyl-accepting chemotaxis protein, respectively. P (proline), C (cysteine), and H (histidine) in each GAF domain show the two corresponding important amino acid residues for the chromophore binding of plant phytochromes. (B and C) Constructs of the two recombinant GST-tagged GAF polypeptides, GST−63k and GST−43k, respectively.

radiation-resistant bacterium *Deinococcus radiodurans* (*7*). Most of these bacteriophytochromes exhibit red/far-red reversible absorption spectral changes similar to those of plant phytochromes upon reconstitution of apoproteins with bilin chromophores *in vitro*.

Both plant phytochromes and bacteriophytochromes can be divided into two functional regions, the N-terminal photosensory region and the C-terminal regulatory region (*8*). The photosensory region senses the light that induces the reversible phototransformation, and the regulatory region is involved in the regulation of light-to-signal transduction. The photosensory region is a bilin lyase domain, a part of which, including the bilin-binding site, is supposed to have a tertiary structure similar to that of GAF, cGMP-binding phosphodiesterase, *Anabaena* adenylate cyclase, and *Escherichia coli* FhlA, domains found in hundreds of signaling and sensory proteins based on amino acid sequence homology (*9*).

Recently, one of us found a novel GAF-containing photoreceptor, PixJ1, in the unicellular cyanobacterium *Synechocystis* sp. PCC 6803 that mediates positive phototactic motility on solid surfaces using a type IV-like pilus structure (*10*−*13*). PixJ1 [entry *sll0041* in Cyanobase (http://www.kazusa.or.jp/cyano/)] contains two GAF domains in addition to a signaling motif found in chemoreceptors, MCP (methyl-accepting chemotaxis protein) (Figure 1A). Purified PixJ1 from *Synechocystis* exhibited a unique reversible phototransformation between a blue light-absorbing (Pb, $\lambda_{Amax} = 435$ nm) form and a green light-absorbing (Pg, $\lambda_{Amax} = 535$ nm) form (*1*). The second GAF domain proved to be the chromophore-binding site on the basis of mutational analyses. A zinc blot following SDS−polyacrylamide gel electrophoresis (PAGE) demonstrated the covalent binding of a tetrapyrrole chromophore.

No such blue−green reversible photoreceptor has been reported so far among the GAF-containing photoreceptors. It is of much interest to clarify the origin of the blue-shifted absorption spectral changes in the GAF domain. There are two possible causes for this blue-shifted spectral change. PixJ1 may bind an unusual bilin chromophore lacking a long-range conjugation system of π-electrons, for example, a rubin-type chromophore, or the π-electron conjugation system is twisted and disrupted within the tertiary structure of the GAF domain. To reveal clues for the molecular basis of this unique photoreversibility, we tried to reconstitute the blue−green reversible phototransformation of the GAF domain in *E. coli* cells that produced a variety of bilins.

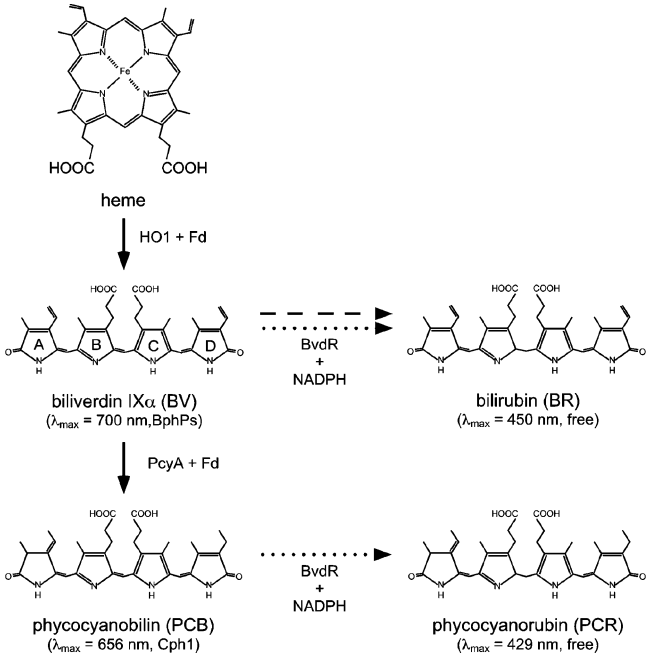

FIGURE 2: Established bilin biogenesis pathways in *Synechocystis* sp. PCC 6803 (arrows with solid lines), a BR synthetic process in animal (arrow with a dashed line), and a proposed BR and PCR synthetic processes in *Synechocystis* sp. PCC 6803 (arrows with dotted lines). Fd means ferredoxin, and for the other abbreviations of the enzymes at each process, see the text. The λ_{max} values of BV and BR are referenced to those of mammal BV and BR (*20*).

All bilin chromophores are derived from heme. The first step is the cleavage of heme at the IXα position by heme oxygenase (HO) to form biliverdin IXα (BV). In plants, BV is converted to phytochromobilin (PΦB), the chromophore of the phytochrome, by phytochromobilin:ferredoxin oxidoreductase (*14*−*17*). In algae and cyanobacteria, BV is converted to phycocyanobilin (PCB) by 3(*Z*)-phycocyanobilin:ferredoxin oxidoreductase (PcyA) (*16*) or to phycoerythrobilin (PEB) by 15,16-dihydrobiliverdin:ferredoxin oxidoreductase, PebA, and 3(*Z*)-phycoerythrobilin:ferredoxin oxidoreductase, PebB (*16*). Algae and cyanobacteria utilize these bilins as light energy-harvesting chromophores in phycobiliproteins (*18*, *19*). PCB is also used as the chromophore for a cyanobacterial phytochrome, Cph1, in *Synechocystis* (*20*). In animals, on the other hand, BV is reduced to bilirubin (BR) by biliverdin reductase (BVR) as part of the degradation pathway of heme (*21*). Plants and higher photosynthetic organisms lack homologues to the BVR gene, while some cyanobacteria, including *Synechocystis*, harbor the gene, *bvdR*. In *Synechocystis*, disruption of the *bvdR* gene was shown to reduce the amount of phycocyanin to an undetectable level, resulting in a 75% reduction in the level of phycobilisome core proteins (*22*). Furthermore, recombinant BvdR of *Synechocystis* was reported to reduce PCB into a phycocyanorubin (PCR)-like bilirubinoid with a λ_{Amax} of 429 nm [$\lambda_{Amax} = 450$ nm in mammalian BR (*23*)], although its activity on PCB was much lower than that on BV (*22*). These results suggest that BR and PCR are synthesized *in vivo* in *Synechocystis*.

Considering the above biosynthetic pathways of bilins in *Synechocystis*, we constructed four expression systems in *E. coli* that produce BV, BR, PCB, and PCR as final products (Figure 2). Using these expression systems, we succeeded in producing GAF-containing polypeptides showing a blue−

green reversible photoreaction almost identical to that of the intact PixJ1.

MATERIALS AND METHODS

Preparation of Bilin-Producing E. coli. Four plasmids, pKT270, *bvdR*/pKT270, pKT271, and *bvdR*/pKT271 for BV, BR, PCB, and PCR synthesis, respectively, were prepared. The pKT270 vector contains the *Synechocystis* HO gene, *ho1* (Cyanobase entry *sll1184*), and pKT271 contains the *ho1* gene and the *Synechocystis* PcyA gene, *pcyA* (Cyanobase entry *slr0116*). These genes were amplified by PCR and sequentially cloned into the pACYC184 vector under the control of a T5 promoter and a lacO operator. The details of the construction of these two plasmids are reported elsewhere (*24*). Two other plasmids, *bvdR*/pKT270 and *bvdR*/pKT271, were prepared as follows. Using the *Synechocystis* genome as a template, DNA fragments corresponding to the *bvdR* gene (Cyanobase entry *slr1784*) were amplified by the PCR method with the following oligonucleotide primers with restriction sites in bold: 5′-**CTCGAG**TAAAGAGGAG-CAAGGTACTATGTCTGAA-3′ and 5′-GCCGAT**GTC-GAC**GCTAATTTTCAACCTTA-3′. The amplified DNA was isolated, digested, and cloned into the pKT270 or pKT271 vector. JM109 strains of *E. coli* were transformed with each vector and used for synthesis of photoactive GAF polypeptides.

Preparation of Recombinant GAF-Containing Polypeptides. Two types of polypeptides containing the second GAF domain of *Synechocystis* sp. PCC 6803 PixJ1 were prepared as N-terminal glutathione *S*-transferase fusion proteins by overexpression the bilin-synthesizing *E. coli* described above. The recombinant polypeptides, GST−43k and GST−63k, were designed as shown in Figure 1, 4- and 20-amino acid extensions at the N-termini and 6- and 170-amino acid extensions at the C-termini of the GAF domain, respectively. Using the *Synechocystis* genome as a template, DNA fragments corresponding to the GAF polypeptides were amplified by the PCR method by using Pfu DNA polymerase (Stratagene, Madison, WI) and the following oligonucleotide primers with restriction sites in bold: 5′-CCAG**GGATC-C**CCGGAAAGCGCCCAGCAAGCC-3′ and 5′-GAGAT-**CTCGAG**TCATGATTCCCCCAATCGCT-3′ for GST−63k and 5′-TAAAGAATTGACT**GGATCC**CCGTCCGCTGC-CATCAACAGC-3′ and 5′-ACTTC**CTCGAG**TCACTGT-TGGGCTAAGAGGTC-3′ for GST−43k. The amplified DNA was isolated, digested, and cloned into pGEX-4T-1 bacterial expression vectors (Amersham Bioscience) as fusion proteins with GST. A linker sequence (Gly-Ser-Pro-Glu-Phe) was inserted to connect the N-terminal end of the polypeptide and the C-terminal end of GST. The two constructs were verified by DNA sequencing with a CEQ 200XL DNA Analysis System (Beckman Coulter). JM109 strains of *E. coli* with the bilin- or rubin-synthesizing genes were transformed with the expression vectors, grown at 310 K in L-broth containing 50 μg/mL ampicillin and 20 μg/mL chloramphenicol until the OD_{600} reached 0.2−0.3, and then incubated in the presence of 0.1 mM isopropyl β-D-thiogalactopyranoside for a further 20 h at 18 °C in the dark. The following purification procedures were carried out at 0−4 °C under dim red light. Harvested bacteria were lysed in phosphate-buffered saline [10 mM Na_2HPO_4, 1.8 mM KH_2PO_4, 140 mM NaCl, and 2.7 mM KCl (pH 7.4)] containing 1 mM phenylmethylsulfonyl fluoride, and the supernatant was mixed and incubated with glutathione−Sepharose 4B gel (Amersham Bioscience). The fusion proteins were eluted from the gel with a solution containing 10 mM reduced glutathione, 50 mM Tris-HCl, 100 mM NaCl, and 1 mM EGTA (pH 7.5).

For the absorption spectral measurements in Figure 4, we substituted the external medium with phosphate-buffered saline. For the denaturation experiment in Figure 5, the GST−43k polypeptide was purified further. The eluted GST−43k polypeptide was applied on a Sephacryl S-100 HR column (Amersham Biosciences) equilibrated and eluted with a solution of 100 mM NaCl, 25 mM Tris-HCl, and 1 mM Na_2EDTA (pH 7.8). The eluted polypeptides were further purified using ion-exchange chromatography with a HiTrap DEAE Sepharose FF column (Amersham Biosciences) and a buffer solution containing 50 mM potassium phosphate and 1 mM Na_2EDTA (pH 6.5) using a gradient from 0 to 1 M NaCl. Elution profiles were monitored by band patterns of Coommasie Brilliant Blue-stained gels after SDS−polyacrylamide gel electrophoresis (PAGE). The fractions containing the fusion proteins were collected and concentrated by ultrafiltration with Centriprep (Millipore). For the zinc-induced fluorescence assay, the SDS−PAGE gel was soaked in 10 mM zinc acetate for 30 min and fluorescence was visualized through a 605 nm filter upon excitation at 532 nm with a FMBIO II system (Hitachi).

Measurements of UV−Visible Absorption Spectra. UV−visible absorption spectra were measured at room temperature (25 °C) with a U-3310 spectrophotometer (Hitachi). For actinic irradiation of the sample solution, violet light (λ_{max} = 400 nm and half-bandwidth of 5 nm at 80 μmol m^{-2} s^{-1}), green light (λ_{max} = 513 nm and half-bandwidth of 30 nm at 30 μmol m^{-2} s^{-1}), and red light (λ_{max} = 640 nm and half-bandwidth of 15 nm at 200 μmol m^{-2} s^{-1}) were provided by the SDL-5N3CUV-A (Sander), DG5306XDG (Stanley Electric), and L645-03AU (Epitex Inc.) light-emitting diodes, respectively.

Urea Denaturation. GST−43k protein in the Pb form purified from *E. coli* coexpressed with pKT271 and *Anabaena cylindrica* phycocyanin (a kind gift of A. Murakami, Kobe University, Kobe, Japan) were prepared in a 50 mM potassium phosphate solution containing 1 mM Na_2EDTA (pH 6.5) with an absorbance of 0.5 at 435 nm and an absorbance of 0.3 at 615 nm, respectively. They were denatured by addition of a 10 M urea solution to give a final urea concentration of 8 M and a pH of 8. After measurements of absorption spectra, the pH of the sample solutions was adjusted to pH 2.0 using HCl and the absorption spectra were remeasured.

In-Gel Digestion and HPLC Analysis. Three excised spots of GST−43k protein separated by SDS−PAGE were subjected to in-gel digestion with trypsin as described in ref *25*, except that the trypsin solution contained 50 mM NH_4HCO_3 and 1 mM $CaCl_2$. Extracted polypeptides from the gel were dried in a centrifugal evaporator and then dissolved in 100 μL of a 0.1% (v/v) TFA and 5% (v/v) acetonitrile solution. After filtration, the polypeptide sample was applied to a Shimadzu LC-10Ai Semi-micro Inert Gradient System and separated on a Macherey-Nagel Nucleosil 120-5C_{18} column (*26*) using a gradient elution of a 0.1% TFA/H_2O solution and a 0.07% TFA/acetonitrile solution at a flow rate

of 0.2 mL/min at room temperature. The elution profile was monitored by the absorbance at 580 and 216 nm, and the eluate was sampled in 0.1 mL fractions. For the experiments described above, HPLC-grade acetonitrile, formic acid, and trifluoroacetic acid (TFA) (Wako Pure Chemical Industry, Osaka, Japan), microselect-grade dithiothreitol and ammonium bicarbonate (Fluka Chemie GmbH, Buchs, Switzerland), and sequencing-grade trypsin (Promega, Madison, WI) were used.

Mass Spectrometry. The HPLC fractions at the main absorption peak at 580 nm were dried in a centrifugal evaporator, resolved in 2 μL of 0.1% TFA and 30% acetonitrile, and analyzed by an AXIMA CFRplus matrix-assisted laser desorption ionization time-of-flight (MALDI-TOF) mass spectrometer (Shimadzu Corp.), using CHCA (α-cyano-4-hydroxycinnamic acid) as a matrix at a concentration of 5 mg/mL CHCA in 0.1% TFA and 50% acetonitrile.

A PCB-bound peptide separated as described above was analyzed using an AXIMA QIT matrix-assisted laser desorption ionization quadrupole ion trap time-of-flight (MALDI-QIT-TOF) mass spectrometer (Shimadzu Corp.) with a matrix of DHB (2,5-dihydroxybenzoic acid). The resultant PCB-desorbed peptide was further analyzed by mass spectrometric peptide fragmentation and sequencing (*25*, *27*) using the AXIMA QIT apparatus (10 mg/mL DHB in 40% acetonitrile). The spectra were calibrated externally using angiotensin II ($[M + H]^+ = 1046.54$) and ACTH fragment ($[M + H]^+ = 2465.20$). MS, MS/MS, and MS/MS/MS spectra were analyzed using Shimadzu Launchpad version 2.4. For the experiments described above, proteomics-recrystallized CHCA and DHB (Wako Pure Chemical Industry) and angiotensin II and ACTH fragment from Sigma-Aldrich (St. Louis, MO) were used.

RESULTS

Synthesis of the GST−GAF Polypeptides in E. coli Harboring Bilin Biosynthesis Genes. To characterize the chromophore in PixJ1, the GAF-containing polypeptides, GST−63k and GST−43k (Figure 1), were synthesized in *E. coli* transformed with genes for the biosynthesis of four different bilins. GAF polypeptides purified by gel filtration and ion-exchange column chromatography were run on SAS−PAGE and analyzed by Coomassie staining and a zinc-induced fluorescence assay.

E. coli transformed with pKT271 and pKT270 carrying the genes for PCB and BV synthesis, respectively, synthesized a GST−63k polypeptide (row 1 of Figure 3A,B) with covalently bound tetrapyrrole (row 2 of Figure 3A,B). These *E. coli* expression systems also synthesized a tetrapyrrole-bound GST−43k polypeptide (data not shown).

The *E. coli* that carries pKT271 and the *bvdR* gene and is expected to synthesize PCR also produced tetrapyrrole-bound GST−43k (rows 1 and 2 of Figure 3C) and GST−63k polypeptides. In contrast, *E. coli* that carries pKT270 and the *bvdR* gene, the genes for BR biosynthesis, produced a GST−63k polypeptide with extremely weak fluorescence (row 1 of Figure 3D), indicating a very low level of covalently bound bilin (row 2 of Figure 3D). Similar results were obtained with GST−43k (data not shown).

The other minor bands that appear in Figure 3, derived possibly from degradation products in the SDS−PAGE, exhibited no Zn-induced tetrapyrrole fluorescence. Since cleavage of GST from GST−63k and GST−43k polypeptides with thrombin resulted in formation of insoluble aggregates, GST fusion proteins were used for the absorption spectroscopy studies below.

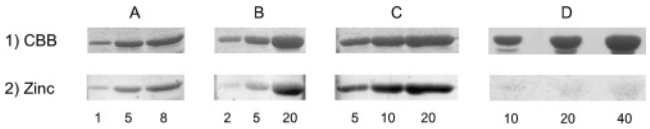

FIGURE 3: Coomassie staining (row 1) and zinc-induced fluorescence (row 2) of the SDS−PAGE bands corresponding to either GST−63k (A, B, and D) or GST−43k (C). Polypeptides were purified from *E. coli* synthesizing PCB (A), BV (B), PCR (C), and BR (D). Numbers below the bands represent the amount in micrograms of the applied GST fusion samples.

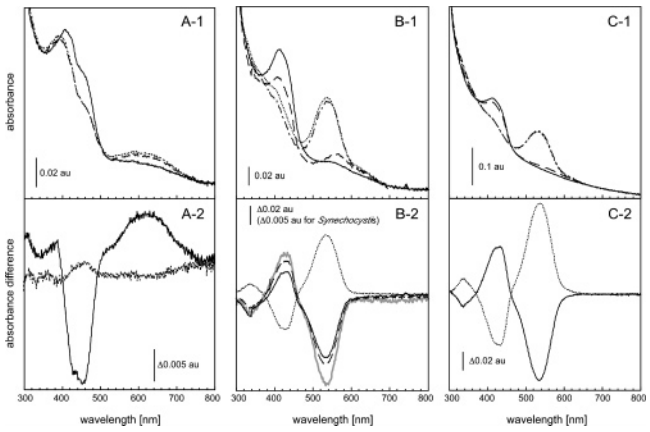

FIGURE 4: UV−visible absorption spectra of the GST−63k and GST−43k polypeptides purified from *E. coli* transformed with BV (A), PCB (B), and PCR (C) biosynthesis genes. (A-1) Absorption spectra of a GST−63k polypeptide from the BV expression system in the dark (solid line, D), after illumination with violet light (dotted line, VL), and after successive illumination with red light (dashed line, RL). (A-2) Absorption difference spectra obtained by VL minus D (solid line) and RL minus VL (dotted line). (B-1) Absorption spectra of the GST−63k polypeptide from the PCB expression system in the dark (solid line, D), after illumination with violet light (dotted line, VL), after successive illumination with green light (dashed line, GL), and after a successive second illumination with violet light (dotted and dashed line, VL2). (B-2) Absorption difference spectra obtained from GL minus VL (dashed line) and VL2 minus GL (dotted line). The solid line and the thick gray line represent the GL minus VL absorption difference spectra of the 43k polypeptide from *E. coli* transformed with PCB and the His-tagged full-length PixJ1 protein isolated from *Synechocystis* sp. PCC 6803 (*1*), respectively. (C-1) Absorption spectra of the GST−43k polypeptide from the PCR expression system. The light conditions of each line are the same as those in panel A-1. (C-2) Absorption difference spectra obtained from GL minus VL (solid line) and VL2 minus GL (dotted line). All the illuminations were saturating.

Spectroscopic Properties of the GST−GAF Polypeptides Synthesized in E. coli Containing Genes for BV and BR Biosynthesis. Spectroscopic properties of the GST−GAF polypeptides produced in *E. coli* transformed with genes for BV and BR biosynthesis were studied. The two bilins have a vinyl substituent at ring A in contrast to an ethylidene substituent in PCB and PCR.

The GST−63k polypeptide isolated from BV-synthesizing *E. coli* bound tetrapyrrole covalently (Figure 3B). The UV−visible absorption spectrum of the GST−63k solution prepared in the dark revealed a peak at 405 nm with a shoulder at around 460 nm overlapping with a large peak in

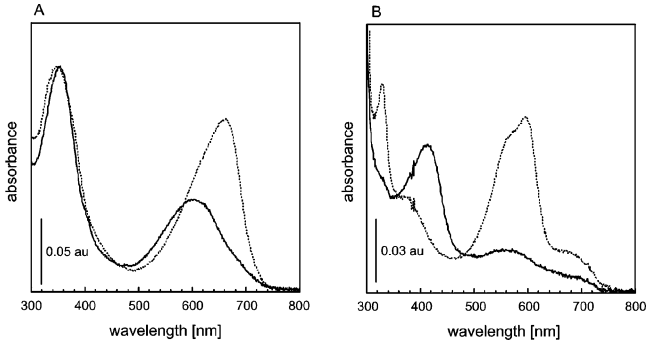

FIGURE 5: UV−visible absorption spectra of (A) *A. cylindrica* phycocyanin and (B) the GST−43k polypeptide purified from *E. coli* transformed with PCB biosynthesis genes, after denaturation with 8 M urea at pH 8.0 (solid line) and pH 2.0 (dotted line).

the UV region (part 1 of Figure 4A, solid line). Illumination with violet light (emission peak at 400 nm) caused an absorbance decrease and a blue shift of the 405 nm absorption peak, and the appearance of a new broad peak spreading from 550 to 650 nm with a λ_{max} at 620 nm (dotted line in part 1 of Figure 4A and solid line in part 2 of Figure 4A). Successive illumination of the new peak with red light (emission peak at 645 nm) changed the spectrum by only a small amount (dashed line in part 1 of Figure 4A and dotted line in part 2 of Figure 4A), indicating that this violet light-induced small absorption change is not reversible.

The GST−GAF polypeptide isolated from *E. coli* that synthesizes BR via BV exhibited a trace amount of covalently bound tetrapyrrole (Figure 3D). In accordance with this result, the absorption spectrum of the GST−63k polypeptide solution exhibited only an obscure absorption peak except for the large absorption by tryptophan in the shorter wavelength region for both the GST−43k and GST−63k polypeptides (data not shown).

Spectroscopic Properties of the GST−GAF Polypeptides Synthesized in E. coli Containing Genes for PCB and PCR Biosynthesis. We studied the spectroscopic properties of the GST−GAF polypeptides prepared in *E. coli*, coexpressed with genes synthesizing PCB and PCR. The two bilins have an ethylidene residue at ring A that enables them to form a thioether linkage with a cysteine in the GAF domains of phytochrome.

The GST−GAF polypeptide produced in the PCB-synthesizing *E. coli* binds a tetrapyrrole chromophore covalently (Figure 3A). The absorption spectrum of a GST−63k solution prepared in the dark exhibited an absorption peak at 410 nm (part 1 of Figure 4B, solid line). Illumination of the sample with violet light induced the appearance of a new absorption peak at 535 nm (part 1 of Figure 4B, dotted line) that reverted after illumination with green light (part 1 of Figure 4B, dashed line). This absorption change was repeatable (part 1 of Figure 4B, dotted and dashed line). The absorption difference spectra revealed a typical reversible photoconversion between the blue light-absorbing form (Pb, λ_{max} = 435 nm) and a green light-absorbing form (Pg, λ_{max} = 535 nm) (part 2 of Figure 4B, solid and dotted line) that is almost identical to Pb (λ_{max} = 435 nm) and Pg (λ_{max} = 535 nm) of His-tagged full-length PixJ1 purified from *Synechocystis* (part 2 of Figure 4B, thick gray line). An absorption difference spectrum of the GST−43k polypeptide prepared in the same PCB-synthesizing *E. coli* was almost the same as that of the GST−63k polypeptide (part 2 of Figure 4B, dashed line), indicating that the amino acid region corresponding to GST−43k is sufficient for the chromophore binding and the reversible blue−green photoconversion of PixJ1, and that the additional N- and C-terminal amino acids in GST−63k do not interfere with either of these functions.

The GST−GAF polypeptide produced in *E. coli* carrying genes for PCR biosynthesis binds bilin covalently (Figure 3C). Their solutions also revealed an almost identical photoreversible conversion between Pb and Pg (part 2 of Figure 4C) almost identical to those of GST−GAF polypeptides prepared by the PCB-synthesizing system (part 2 of Figure 4B).

Absorption Spectra of the Denatured GST−43k Polypeptide and Phycocyanin. Since GST−GAF polypeptides prepared in the PCB-synthesizing *E. coli* mimic well the blue−green spectral change of the full-length PixJ1, denaturation effects on the absorption spectra were studied with the GST−43k polypeptide. Among the phycobiliproteins in cyanobacteria, phycocyanin and allophycocyanin are known to bind PCB covalently as the chromophore (*18*, *28*). The biliproteins in the native state show a broad range of λ_{max} from 615 to 650 nm in their first absorption band (*18*). However, in the acidic urea solutions that minimize the effect of the apoprotein on the absorption spectra of the chromophore, the λ_{max} of the first absorption band comes to around 660 nm (*29*, *30*) and its molar extinction coefficient increases. Therefore, the absorption spectra of the GST−43k polypeptide were compared with those of phycocyanin from *A. cylindrica* in the acidic urea solution.

The absorption spectrum of the phycocyanin in a 8.0 M urea solution at pH 8.0 exhibited two absorption peaks with a λ_{max} at 350 and 600 nm (Figure 5A, solid line). The λ_{max} of the first absorption band shifted from 600 to 663 nm, and the extinction coefficient increased at pH 2.0 (Figure 5A, dotted line). The GST−43k polypeptide thought to bind PCB exhibited a second absorption peak at 408 nm and a broad first absorption band at around 560 nm in 8 M urea at pH 8.0 (Figure 5B, solid line). At pH 2.0, the first absorption peak exhibited an increase in the extinction coefficient but showed only a small red shift to 595 nm with a shoulder at 568 nm (Figure 5A, dotted line). In addition, a broad new peak appeared at around 660 nm that increased in magnitude and was accompanied by a decrease in the magnitude of the 595 nm peak when the GST−43k polypeptide solution was left in the dark at room temperature (data not shown).

Isolation of the Chromopeptide from the GST−GAF Polypeptide. To obtain the information concerning the chromophore and its binding site in the GAF polypeptide by MS, we isolated chromopeptides from tryptic fragments of the GST−43k polypeptide by HPLC. The HPLC elution profile detected by 580 nm exhibited a single large peak at a retention time of ∼38 min and a few very small peaks (Figure 6A). The major peak (arrow) was collected and used for MS analysis.

Analysis by Mass Spectrometry. The collected chromopeptide was applied on a MALDI-TOF mass spectrometer. The monoisotopic masses showed four major ion signals at *m*/*z* 2269.23, 2326.26, 2357.30, and 2929.54. Among the four signals, that at *m*/*z* 2929.54 (Figure 6B) matched well the calculated mass, 2929.50, of PCB with a peptide with the DIYNAGLTPCHIGQLKPFEVK amino acid sequence that

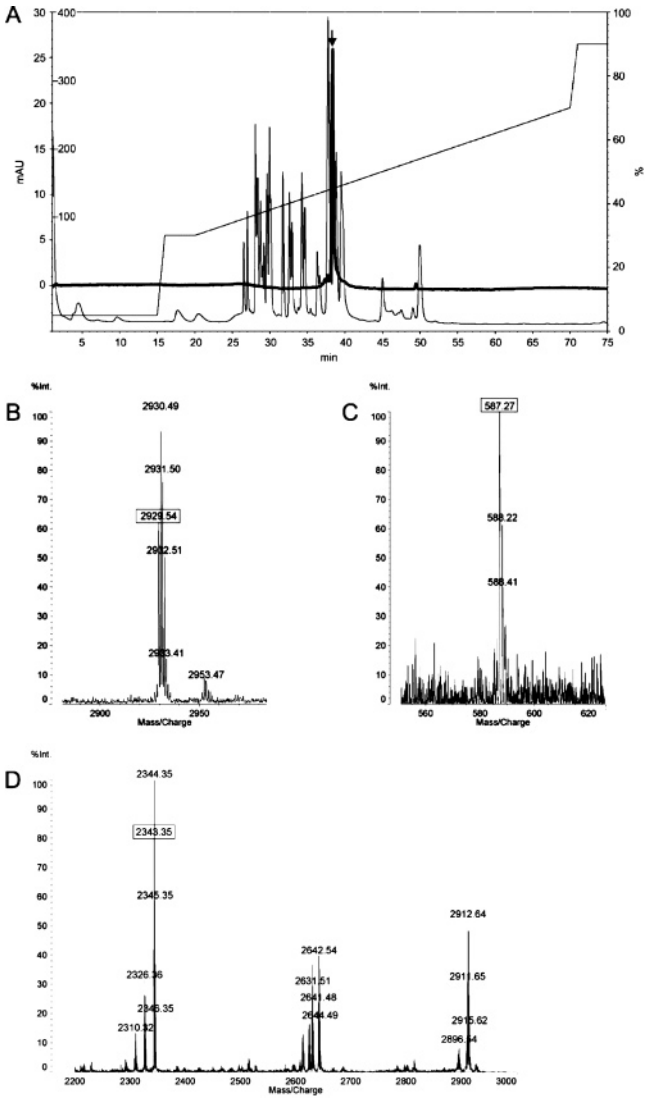

FIGURE 6: (A) HPLC elution profile of tryptic fragments of the GST−43k polypeptide. The absorptions at 580 nm (thick trace) and 216 nm (thin trace) and the gradient used for the elution (thin linear line) are indicated. The gradient is shown as the percentage of a 0.07% TFA/acetonitrile solution in a 0.1%TFA/H_2O solution. mAU indicates milliabsorbance unit. The arrow shows the main chromopeptide peak. (B and C) MALDI-TOF MS of the chromopeptide shown in panel A by the arrow. (B) MS spectrum around the ion signal at *m*/*z* 2929.54 (box) corresponding to the calculated mass, 2929.50, of a PCB-bearing peptide with the DIYNAGLTPCHIGQLKPFEVK amino acid sequence, including the chromophore-binding motif of cysteine-histidine in the GAF polypeptide. (C) MS spectrum around the in-source decay (ISD) ion signal at *m*/*z* 587.27 corresponding to the calculated mass, 587.29, of PCB. (D) MS/MALDI-QIT-TOF MS spectrum of the peptide with ion signal at *m*/*z* 2929.54 in the MS (Figure 6B, box). The main signal at *m*/*z* 2343.35 corresponding to the calculated mass, 2343.38, of the 21-amino acid DIYNAGLTPCHIGQLKPFEVK peptide without PCB is indicated with a box.

covers the chromophore-binding motif of cysteine-histidine in the GAF polypeptide. Furthermore, in the low-*m*/*z* region, we detected an in-source decay (ISD) ion signal at *m*/*z* 587.27 (Figure 6C), which is almost identical to the calculated mass, 587.29, for PCB, suggesting that the signal comes from the desorbed chromophore.

The peptide producing an ion signal at *m*/*z* 2929.54 (Figure 6B, box) was subjected to MALDI-QIT-TOF mass spectrometry. The main MS/MS signal at *m*/*z* 2343.35 (Figure 6D, box) coincides with the calculated mass, 2343.38, of the 21-amino peptide without PCB, indicating that the signal comes from the peptide after desorption of PCB. This peptide was further subjected to MS/MS/MS analysis and sequencing. The spectrum (Figure 7) exhibited intense collision-induced dissociation (CID) fragment ion signals from both the Y-type and B-type ion series (*27*) as well as the other ions derived from additional fragmentations such as the loss of H_2O and of ammonia. The partial amino acid sequence, DIYNAGLTPCHIGQLKPFEVK, determined from the MS/MS/MS spectrum is identical to that of the 21-amino acid polypeptide proposed on the basis of the mass data. The mass analysis data clearly show that the chromophore, probably PCB, binds to the 21-amino acid sequence region that includes the cysteine-histidine motif of phytochrome chromophore binding.

DISCUSSION

Reconstitution of a Reversible Photoconversion between Pb and Pg in the Bilin-Bound GAF Polypeptides. Previously, the His-tagged full-length PixJ1 expressed and isolated from the *Synechocystis* cells was found to bind a bilin chromophore(s) covalently in only the second GAF domain and to exhibit a photoreversible conversion between two distinct absorption forms, Pb and Pg (*1*). Since the molecular species of the chromophore was not identified in that study, we tried to reconstitute the GAF polypeptides with a variety of bilin chromophores *in vitro*. However, we obtained an extremely low reconstitution yield using the standard method of mixing DMSO or MeOH solutions of bilins with the GAF polypeptides as compared with plant phytochrome (*31*) or bacteriophytochromes (*4*−*7*). We, therefore, used the *in vivo* reconstitution method.

In the study presented here, almost the same photoconversion was successfully reproduced in the GST fusion polypeptides with the second GAF domains that were coexpressed with genes for synthesis of PCB or PCR (Figure 4).

Molecular Species of the Chromophore Responsible for a Reversible Photoconversion between Pb and Pg. *E. coli* transformed with pKT271 can produce two bilin pigments, BV and PCB. Since the GST−GAF polypeptides from the BV-synthesizing system did not show the blue−green photoconversion even though the polypeptides could bind to the chromophore (Figure 4A), it is reasonably concluded that PCB is the chromophore responsible for this photoconversion, although a possible modification of PCB in the *E. coli* cell cannot be excluded completely. *E. coli* transformed with *bvdR*/pKT271 can produce four bilin pigments, BV, BR, PCB, and PCR. BV can be excluded as a candidate for the target chromophore as described above. Furthermore, the GAF polypeptides prepared from BR-synthesizing *E. coli* bind no bilin as proved by the zinc staining analysis (row 2 of Figure 3D). Between the remaining two chromophores, PCB and PCR, PCB is very likely to be responsible for the spectral changes on the basis of the following two facts. First, plant phytochrome that has the same amino acid sequence, cysteine-histidine for chromophore binding, has been reported to bind PCB and a trace amount of BV but not BR nor PCR *in vitro* (*32*). Second, recombinant BvdR of *Synechocystis* was reported to exhibit a 10 times lower

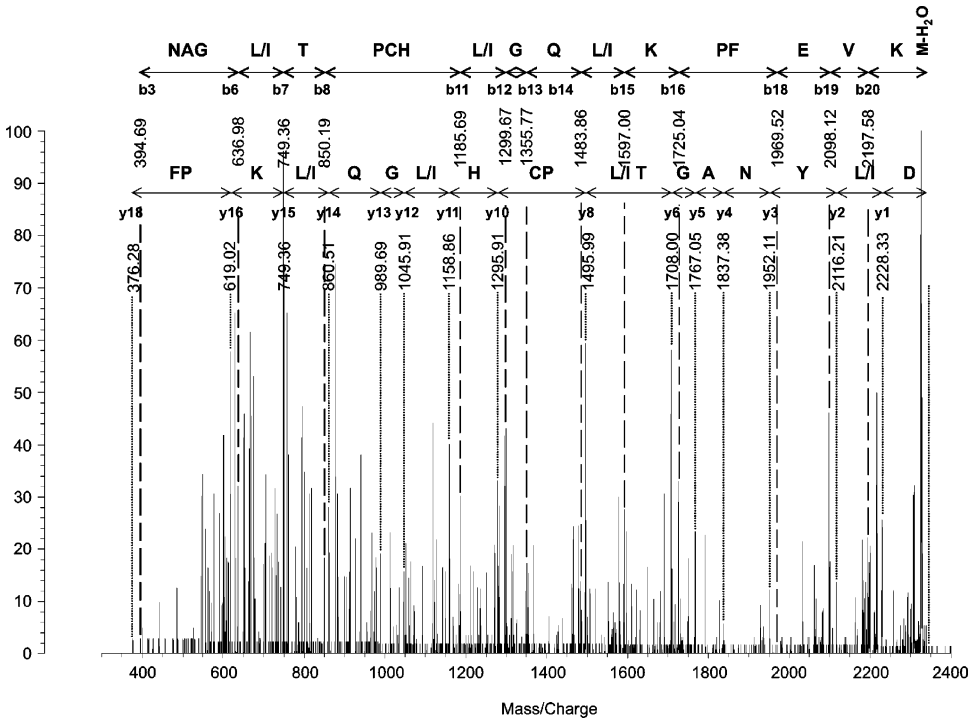

FIGURE 7: MS/MS/MALDI-QIT-TOF MS spectrum of the peptide with an ion signal at *m*/*z* 2343.35 in the MS/MS spectrum (Figure 6D, box). The mass spectrometric fragment ions from both the Y-type and B-type ion series are indicated. The determined partial amino acid sequence is depicted and was assigned to the 21-amino acid peptide DIYNAGLTPCHIGQLKPFEVK in the GAF polypeptide.

reductase activity on PCB than on BV (*22*). Thereafter, PCB may accumulate as an intermediate product due to the low activity of BvdR on PCB in the *E. coli* cells and may be bound to the GAF polypeptides. The PCB-bound polypeptides can be the origin for the observed spectral changes. Actually, the spectral changes of the GAF polypeptides are almost indistinguishable between the pKT271 and *bvdR*/pKT271 systems (Figure 4), suggesting that the GAF polypeptides from different expression systems bind the same chromophore to each other.

MS detected the signal coming from the desorbed chromophore that has the calculated mass of PCB, supporting the idea that PCB is the chromophore. However, these data should be treated with care since the difference in mass between PCB and PCR is only 2 and is within the mass variation coming from different ionized states or different binding modes from a thioether bonding of PCR. The absorption spectrum of the trypsin-digested GST−43K polypeptide after treatment with SDS−PAGE sample buffer exhibited a λ_{max} at 555 nm, which is almost the same as that of phycocyanin from *A. cylindrica* (560 nm, data not shown). The data indicate that the attached chromophore has an extended π-electron conjugation system like PCB but not rubin-type linear tetrapyrrole lacking the conjugation between the B and C rings. Thus, all the results can be reasonably explained by the interpretation that PCB is the chromophore responsible for the reversible photoconversion between Pb and Pg.

Chromophore-Binding Site. PCB has an ethylidene side chain at ring A that is known to attach to a conserved cysteine in the GAF domains of plant and some cyanobacterial phytochromes. BV has, on the other hand, a vinyl side chain at ring A, which is shown to be responsible for the chromophore binding of the bacteriophytochromes from *Agrobacterium* Agp1 and *D. radiodurans* DrBphP. Some other bacteriophytochromes from *Pseudomonas syringae* PsBphP, *Bradyrhizobium* BrBphP, or *Calothrix* CphB also bind BV covalently, but the binding rings have not been resolved (*7*, *33*−*35*). Agp1 and DrBphP bind BV at an N-terminal cysteine which is far from the chromophore-binding region of phytochromes (*6*, *36*−*38*). The recently determined crystal structure of DrBphP shows the binding of A ring $C3^2$ to the thiol group of the cysteine which is different from the binding at $C3^1$ in the ethylidene-type chromophore (*38*). This N-terminal cysteine is well-conserved among bacteriophytochromes lacking the conserved cysteine in their GAF domains. On the other hand, none of all the plant phytochromes and only some of the cyanobacterial phytochromes carrying a chromophore in GAF domains have the N-terminal cysteine. From this point of view, PixJ1 falls into the latter (plant) type phytochrome, since it carries a cysteine at the second GAF domain responsible for chromophore binding (*1*). These MS data proved that the chromophore, probably PCB, binds to the 21-amino acid region, DIYNAGLTPCHIGQLKPFEVK, of the GAF polypeptide, including the conserved cysteine.

Molecular Basis for the Blue-Shifted Absorption Spectral Change. In contrast to the plant phytochromes that bear PΦB as the chromophore, prokaryotic phytochrome-like photoreceptors have been known to bind other bilins, such as PCB in *Synechocystis* Cph1 (*20*) and BV in bacterial BphP from *Bradyrhizobium* due to the lack of PΦB biosynthetic pathways. *In vitro* assembly experiments have also shown the binding of PCB by CphA from the cyanobacterium *Calothrix* PCC 7601 (*5*) or binding of BV by CphB from *Calothrix* (*20*), and BphPs from *P. aeruginosa* and *D. radiodurans* (*7*). All these bacterial phytochromes, however, exhibit a similar photoconversion between Pr and Pfr. The

photoconversion between Pb and Pg of PixJ1 is very unique, and the underlying molecular mechanism for this blue shift is of great interest.

An absorption maximum of UV−visible spectra of bilins is determined by its π-electron conjugation system as well as the structure of its binding pocket in biliproteins. Verdin-type bilins, such as BV, PCB, and PΦB, have extended π-electron conjugation systems from ring A to D that are responsible for the photoconversion between Pr and Pfr in the GAF domains. On the other hand, three bilins with disrupted conjugation systems have been reported to show blue-shifted absorption maxima in biliproteins. PEB that lacks the π-electron conjugation between rings C and D exhibits the absorption maxima in the wavelength region from 540 to 575 nm in the free forms, and those from 535 to 567 nm after binding to phycobilisome proteins (*18*). PEB carries an ethylidene side chain at ring A and is bound to a conserved cysteine in plant phytochromes through a thioether linkage with a λ_{max} of 575 nm, although it is not photoconvertible (*32*, *39*). Since *Synechocystis* does not synthesize PEB, it cannot be responsible for this blue−green photoconversion. Phycourobilin (PUB) lacking the conjugation between rings A and B in addition to that between rings C and D has a λ_{max} at 495 nm in phycobiliproteins (*40*). The biosynthetic pathway of PUB is not known, but its involvement in this phototransformation can be excluded since PUB has not been detected in *Synechocystis*. The third bilin, phycoviolobilin (PVB), missing the conjugation between rings A and B shows an absorption maximum at 568 nm in the α-subunit of phycoerythrocyanin (PecA) (*41*). The biosynthetic pathway of this bilin is still not clear. In the cyanobacterium *Mastigocladus*, PecE and PecF, which are homologues of CpcE and CpcF of PCB lyase, respectively, catalyze the covalent attachment of PCB to PecA and isomerization and reduction of PCB to PVB (*41*, *42*). PVB is bound to a cysteine in PecA via thioether bond and shows a reversible photoconversion between a 505 and 570 nm-absorbing form that comes from *Z*/*E* photoisomerization around the C_{15}═C_{16} bond between rings C and D (*43*, *44*). In *Synechocystis*, however, PVB-attached biliproteins have not been detected. Furthermore, the *Synechocystis* genome harbors CpcE and CpcF genes but no genes obviously homologous to PecE and PecF. Accordingly, the involvement of PVB in this photoconversion may be excluded. Rubin-type bilins, such as BVR and PCR, also show a blue-shifted absorption, but their contributions to this blue−green photoconversion can be excluded as discussed in the previous section. All these are consistent with the results presented here and indicate PCB is the chromophore responsible for Pb−Pg phototransformation.

Accordingly, the molecular structure of the bilin-binding pocket is likely a key factor for Pb−Pg phototransformation. For example, the Archaeon *Halobacterium salinarum* has four retinal binding proteins, bacteriorhodopsin (*45*), halorhodopsin (*46*), sensory rhodopsin I (*47*), and phoborhodopsin (pR) or sensory rhodopsin II (*48*). All of them bind retinal as the chromophore and are in an all-trans form in the ground state; however, the former three have λ_{max} in the wavelength region of 560−590 nm, while pR shows a λ_{max} of $<$500 nm (*49*). The blue-shifted λ_{max} of pR is supposed to be caused by the different structure in the retinal-binding pocket.

In this analogy, PCB in the binding pocket of the GAF polypeptides might disrupt its π-electron conjugation system by twisting the planar configuration, and/or the π-electron might be localized due to the electrostatic interactions with a cationic amino acid residue(s). Since even the disruption of the two π-electron conjugations between rings A and B and between rings C and D shifts the λ_{max} only to ∼500 nm (*40*), both contributions seem to be required to shift the λ_{Amax} of Pb to 430 nm. To keep the PCB in such an unusual configuration in the binding pocket, PCB may need to attach to the apoprotein at two positions. In fact, some phycobiliproteins have been shown to bind bilins via two linkages; the β-subunit of *Gastroclonium coulteri* R phycoerythrin binds PUB at ring A and ring D covalently (*40*).

This view may be supported by the results of denaturation treatment of the GAF polypeptide (Figure 5). The 8 M urea treatment at pH 2.0 of phycocyanin that uncovers the effect of the protein moiety on PCB produces a typical denatured spectrum with a peak at 663 nm with an increased molar extinction coefficient. In the GAF polypeptide, however, the treatment gave a spectrum different from that of phycocyanin. The GAF polypeptide still has a λ_{max} at 595 nm in the acidic urea solution that decreases in magnitude and is accompanied by a gradual increase in the magnitude of a peak at 670 nm corresponding to that of the naked PCB in phycocyanin. This indicates the existence of strong interactions between the bilin and apoprotein even in the acidic urea solution. Interestingly, the absorption spectrum of the GST−GAF polypeptide in the acidic urea is very similar to that of PecA having PVB as the chromophore in the acidic urea solution (compare Figure 5B with Figure 2 of ref *43*). The similar absorption spectra of the GAF polypeptide and PecA in the acidic urea solution indicate that the GAF chromophore has a π-electron conjugation similar to that of the PecA chromophore in the naked state. Since PVB lacks the π-electron conjugation between rings A and B, the bilin chromophore of the GAF polypeptide preserves a similar configuration in which the π-electron conjugation between rings A and B is inhibited even under the crucial condition. To keep this configuration, a two-covalent bonding, possibly via rings A and B or rings A and C, of the chromophore to the apoprotein is very probable.

The difference between the λ_{max} of Pb and Pg is 100 nm, which is somewhat larger than those of ∼60 nm of PΦB in plant phytochromes, 50 nm of PCB in *Synechocystis* Cph1, or 65 nm of PVB in PecA; however, it could be explained by *Z*/*E* photoisomerization around a double bond, possibly between rings C and D as observed with known photoreceptors with linear tetrapyrrole chromophores. To elucidate the molecular processes underlying this unique photoconversion, we need to conduct further studies such as crystallography (*38*) or detailed *in vitro* reconstitution studies as reported with phytochrome B (*50*).

ACKNOWLEDGMENT

Thanks are due to Dr. A. Murakami at Kobe University for supplying us with *A. cylindrica* phycocyanin, Dr. C. Kami at Nara Institute of Science and Technology for the use of FMBIO, Ms. T. Konishi for her technical assistance, and Dr. M. Terry at University of Southampton for English revision of the manuscript.

REFERENCES

1. Yoshihara, S., Katayama, M., Geng, X., and Ikeuchi, M. (2004) Cyanobacterial phytochrome-like PixJ1 holoprotein shows novel reversible photoconversion between blue- and green-absorbing forms, *Plant Cell Physiol. 45*, 1729−1737.
2. Smith, H. (2000) Phytochromes and light signal perception by plants: An emerging synthesis, *Nature 407*, 585−591.
3. Quail, P. H. (2002) Phytochrome photosensory signalling networks, *Nat. Rev. Mol. Cell Biol. 3*, 85−93.
4. Hughes, J., Lamparter, T., Mittmann, F., Hartmann, E., Gärtner, W., Wilde, A., and Börner, T. (1997) A prokaryotic phytochrome, *Nature 386*, 663.
5. Jorissen, H. J., Quest, B., Remberg, A., Coursin, T., Braslavsky, S. E., Schaffner, K., Tandeau de Marsac, N., and Gartner, W. (2002) Two independent, light-sensing two-component systems in a filamentous cyanobacterium, *Eur. J. Biochem. 269*, 2662−2671.
6. Lamparter, T., Michael, N., Mittmann, F., and Esteban, B. (2002) Phytochrome from *Agrobacterium tumefaciens* has unusual spectral properties and reveals an N-terminal chromophore attachment site, *Proc. Natl. Acad. Sci. U.S.A. 99*, 11628−11633.
7. Davis, S. J., Vener, A. V., and Vierstra, R. D. (1999) Bacteriophytochromes: Phytochrome-like photoreceptors from nonphotosynthetic eubacteria, *Science 286*, 2517−2520.
8. Montgomery, B. L., and Lagarias, J. C. (2002) Phytochrome ancestry: Sensors of bilins and light, *Trends Plant Sci. 7*, 357−366.
9. Aravind, L., and Ponting, C. P. (1997) The GAF domain: An evolutionary link between diverse phototransducing proteins, *Trends Biochem. Sci. 22*, 458−459.
10. Bhaya, D., Bianco, N. R., Bryant, D., and Grossman, A. (2000) Type IV pilus biogenesis and motility in the cyanobacterium *Synechocystis* sp. PCC6803, *Mol. Microbiol. 37*, 941−951.
11. Yoshihara, S., Suzuki, F., Fujita, H., Geng, X. X., and Ikeuchi, M. (2000) Novel putative photoreceptor and regulatory genes required for the positive phototactic movement of the unicellular motile cyanobacterium *Synechocystis* sp. PCC 6803, *Plant Cell Physiol. 41*, 1299−1304.
12. Yoshihara, S., Geng, X., Okamoto, S., Yura, K., Murata, T., Go, M., Ohmori, M., and Ikeuchi, M. (2001) Mutational analysis of genes involved in pilus structure, motility and transformation competency in the unicellular motile cyanobacterium *Synechocystis* sp. PCC 6803, *Plant Cell Physiol. 42*, 63−73.
13. Okamoto, S., and Ohmori, M. (2002) The cyanobacterial PilT protein responsible for cell motility and transformation hydrolyzes ATP, *Plant Cell Physiol. 43*, 1127−1136.
14. Terry, M. J., McDowell, M. T., and Lagarias, J. C. (1995) (3*Z*)- and (3*E*)-phytochromobilin are intermediates in the biosynthesis of the phytochrome chromophore, *J. Biol. Chem. 270*, 11111−11118.
15. Wu, S. H., McDowell, M. T., and Lagarias, J. C. (1997) Phycocyanobilin is the natural precursor of phytochrome from the green alga *Mesotaenium caldariorum*, *J. Biol. Chem. 272*, 25700−25705.
16. Frankenberg, N., Mukougawa, K., Kohchi, T., and Lagarias, J. C. (2001) Functional genomic analysis of the HY2 family of ferredoxin-dependent bilin reductases from oxygenic photosynthetic organisms, *Plant Cell 13*, 965−978.
17. Kohchi, T., Mukougawa, K., Frankenberg, N., Masuda, M., Yokota, A., and Lagarias, J. C. (2001) The *Arabidopsis* HY2 gene encodes phytochromobilin synthase, a ferredoxin-dependent biliverdin reductase, *Plant Cell 13*, 425−436.
18. Glazer, A. N. (1988) Phycobiliproteins, *Methods Enzymol. 167*, 291−303.
19. Beale, S. I. (1994) Biosynthesis of open-chain tetrapyrroles in plants, algae, and cyanobacteria, *Ciba Found. Symp. 180*, 156−168, 168−171 (discussion).
20. Hübschmann, T., Börner, T., Hartmann, E., and Lamparter, T. (2001) Characterization of the Cph1 holo-phytochrome from *Synechocystis* sp. PCC 6803, *Eur. J. Biochem. 268*, 2055−2063.
21. Foresti, R., Green, C. J., and Motterlini, R. (2004) Generation of bile pigments by haem oxygenase: A refined cellular strategy in response to stressful insults, *Biochem. Soc. Symp.*, 177−192.
22. Schluchter, W. M., and Glazer, A. N. (1997) Characterization of cyanobacterial biliverdin reductase. Conversion of biliverdin to bilirubin is important for normal phycobiliprotein biosynthesis, *J. Biol. Chem. 272*, 13562−13569.
23. Maines, M. D., and Trakshel, G. M. (1993) Purification and characterization of human biliverdin reducatse, *Arch. Biochem. Biophys. 300*, 320−326.
24. Mukougawa, K., Kanamoto, H., Kobayashi, T., Yokota, A., and Kohchi, T. (2006) Metabolic engineering to produce phytochromes with phytochromobilin, phycocyanobilin, or phycoerythrobilin chromophore in *Escherichia coli*, *FEBS Lett.* (in press).
25. Koy, C., Mikkat, S., Raptakis, E., Sutton, C., Resch, M., Tanaka, K., and Glocker, M. O. (2003) Matrix-assisted laser desorption/ionization- quadrupole ion trap-time of flight mass spectrometry sequencing resolves structures of unidentified peptides obtained by in-gel tryptic digestion of haptoglobin derivatives from human plasma proteomes, *Proteomics 3*, 851−858.
26. Sanderson, K., Thornwall, M., Nyberg, G., Glamsta, E. L., and Nyberg, F. (1994) Reversed-phase high-performance liquid chromatography for the determination of haemorphin-like immunoreactivity in human cerebrospinal fluid, *J. Chromatogr., A 676*, 155−160.
27. Roepstorff, P., and Fohlman, J. (1984) Proposal for a common nomenclature for sequence ions in mass spectra of peptides, *Biomed. Mass Spectrom. 11*, 601.
28. Glazer, A. N. (1989) Light guides. Directional energy transfer in a photosynthetic antenna, *J. Biol. Chem. 264*, 1−4.
29. Glazer, A. N., and Fang, S. (1973) Chromophore content of blue-green algal phycobiliproteins, *J. Biol. Chem. 248*, 659−662.
30. Glazer, A. N., and Hixson, C. S. (1975) Characterization of R-phycocyanin. Chromophore content of R-phycocyanin and C-phycoerythrin, *J. Biol. Chem. 250*, 5487−5495.
31. Elich, T. D., and Lagarias, J. C. (1989) Formation of a photoreversible phycocyanobilin-apophytochrome adduct *in vitro*, *J. Biol. Chem. 264*, 12902−12908.
32. Li, L., and Lagarias, J. C. (1992) Phytochrome assembly. Defining chromophore structural requirements for covalent attachment and photoreversibility, *J. Biol. Chem. 267*, 19204−19210.
33. Bhoo, S. H., Davis, S. J., Walker, J., Karniol, B., and Vierstra, R. D. (2001) Bacteriophytochromes are photochromic histidine kinases using a biliverdin chromophore, *Nature 414*, 776−779.
34. Giraud, E., Fardoux, J., Fourrier, N., Hannibal, L., Genty, B., Bouyer, P., Dreyfus, B., and Vermeglio, A. (2002) Bacteriophytochrome controls photosystem synthesis in anoxygenic bacteria, *Nature 417*, 202−205.
35. Quest, B., and Gartner, W. (2004) Chromophore selectivity in bacterial phytochromes: Dissecting the process of chromophore attachment, *Eur. J. Biochem. 271*, 1117−1126.
36. Lamparter, T., Carrascal, M., Michael, N., Martinez, E., Rottwinkel, G., and Abian, J. (2004) The biliverdin chromophore binds covalently to a conserved cysteine residue in the N-terminus of *Agrobacterium* phytochrome Agp1, *Biochemistry 43*, 3659−3669.
37. Lamparter, T., Michael, N., Caspani, O., Miyata, T., Shirai, K., and Inomata, K. (2003) Biliverdin binds covalently to *Agrobacterium* phytochrome Agp1 via its ring A vinyl side chain, *J. Biol. Chem. 278*, 33786−33792.
38. Wagner, J. R., Brunzelle, J. S., Forest, K. T., and Vierstra, R. D. (2005) A light-sensing knot revealed by the structure of the chromophore-binding domain of phytochrome, *Nature 438*, 325−331.
39. Murphy, J. T., and Lagarias, J. C. (1997) The phytofluors: A new class of fluorescent protein probes, *Curr. Biol. 7*, 870−876.
40. Klotz, A. V., and Glazer, A. N. (1985) Characterization of the bilin attachment sites in R-phycoerythrin, *J. Biol. Chem. 260*, 4856−4863.
41. Zhao, K. H., Wu, D., Wang, L., Zhou, M., Storf, M., Bubenzer, C., Strohmann, B., and Scheer, H. (2002) Characterization of phycoviolobilin phycoerythrocyanin-α 84-cystein-lyase-(isomerizing) from *Mastigocladus laminosus*, *Eur. J. Biochem. 269*, 4542−4550.
42. Storf, M., Parbel, A., Meyer, M., Strohmann, B., Scheer, H., Deng, M. G., Zheng, M., Zhou, M., and Zhao, K. H. (2001) Chromophore attachment to biliproteins: Specificity of PecE/PecF, a lyase-isomerase for the photoactive 3(1)-Cys-α 84-phycoviolobilin chromophore of phycoerythrocyanin, *Biochemistry 40*, 12444−12456.
43. Zhao, K. H., Haessner, R., Cmiel, E., and Scheer, H. (1995) Type I reversible photochemistry of phycoerythrocyanin involves Z/E-isomerization of α-84 phycoviolobilin chromophore, *Biochim. Biophys. Acta 1228*, 235−243.

44. Zhao, K. H., and Scheer, H. (1995) Type I and type II reversible photochemistry of phycoerythrocyanin a-subunit from *Mastigocladus laminosus* both involve Z, E isomerization of phycoviolobilin chromophore and are controlled by sulfhydryls in apoprotein, *Biochim. Biophys. Acta 1228*, 244−253.
45. Oesterhelt, D., and Stoeckenius, W. (1971) Rhodopsin-like protein from the purple membrane of *Halobacterium halobium*, *Nat. New Biol. 233*, 149−152.
46. Varo, G. (2000) Analogies between halorhodopsin and bacteriorhodopsin, *Biochim. Biophys. Acta 1460*, 220−229.
47. Bogomolni, R. A., and Spudich, J. L. (1982) Identification of a third rhodopsin-like pigment in phototactic *Halobacterium halobium*, *Proc. Natl. Acad. Sci. U.S.A. 79*, 6250−6254.
48. Takahashi, T., Tomioka, H., Kamo, N., and Kobatake, Y. (1985) A photosystem other than PS370 also mediates the negative phototaxis of *Halobacterium halobium*, *FEMS Microbiol. Lett. 28*, 161−164.
49. Takahashi, T., Yan, B., Mazur, P., Derguini, F., Nakanishi, K., and Spudich, J. L. (1990) Color regulation in the archaebacterial phototaxis receptor phoborhodopsin (sensory rhodopsin II), *Biochemistry 29*, 8467−8474.
50. Hanzawa, H., Shinomura, T., Inomata, K., Kakiuchi, T., Kinoshita, H., Wada, K., and Furuya, M. (2002) Structural requirement of bilin chromophore for the photosensory specificity of phytochromes A and B, *Proc. Natl. Acad. Sci. U.S.A. 99*, 4725−4729.

BI051983L